FINITE ELEMENT ANALYSIS OF THE BEHAVIOUR OF REINFORCED CONCRETE COLUMNS CONFINED BY OVERLAPPING HOOPS SUBJECTED TO RAPID CONCENTRIC LOADING

Xiang Zeng[1, 2]

1. *College of Civil Engineering and Architecture, Hainan University, No.58, Renmin Ave., Haikou 570228, China*
   Hainan Institute of Development on International Tourist Destination, No.58, Renmin Ave., Haikou 570228, China; E-mail: zengxce@hainu.edu.cn

ABSTRACT

The strain rate sensitivity of concrete material was discovered approximately one hundred years ago, and it has a marked effect on the behaviour of concrete members subjected to dynamic loadings such as strong earthquake and impact loading. Because of the great importance of the confined reinforced concrete (RC) columns in RC structures, the dynamic behaviour of the columns induced by the strain rate effect has been studied, but only few experiments and analyses have been conducted. To investigate the behaviour of overlapping hoop-confined square reinforced normal-strength concrete columns, considering the strain rate effect at a strain rate of 10^{-5}/sec to 10^{-1}/sec induced by earthquake excitation, an explicit dynamic finite element analysis (FEA) model was developed in ABAQUS to predict the behaviour of confined RC columns subjected to the rapid concentric loading. A locally modified stress-strain relation of confined concrete with the strain rate sensitivity of the concrete material and the confining effect of overlapping hoops were proposed to complete the simulation of the dynamic behaviour of concrete with the concrete plastic-constitutive model in ABAQUS. The finite element predictions are consistent with the existing test results. Based on the FEA model, a parametric investigation was conducted to capture more information about the behaviour of confined RC columns under varying loading rates.

KEYWORDS

Reinforced concrete columns, Rapid loading, Overlapping hoops, Confining effect, Strain rate sensitivity, Finite element analysis, Parametric investigation

INTRODUCTION

With the increasing strain rate of concrete and reinforcing steel, the properties of these materials change. This refers to the strain rate sensitivity of concrete and reinforcing steel, which has been documented in literature [1-5]. The strain rate sensitivity of the materials significantly affects the behaviour of reinforced concrete (RC) members under dynamic loading. As a typical type of dynamic load, earthquake loading induces strain rates on the structures. The quasi-static stain rate is commonly approximately 10^{-6}/sec to 10^{-5}/sec. Bertero predicted that for a notably rigid RC structure with a fundamental natural period of approximately 0.1 s under earthquake action, the strain rate at some critical regions can be as high as 0.025/sec [6]. Generally, the strain rate of materials in RC structures under earthquake loading is approximately from 10^{-4}/sec to 10^{-1}/sec [7-9]. Asprone et al. conducted an earthquake evaluation analysis of RC structures to appreciate the effect of the strain rate sensitivity of concrete and reinforcing steel on the global seismic response of RC structures [10]. The result shows that considering the updated material properties, to

----

account for the earthquake-induced strain rate, a strength reserve of the structural system is experienced when only ductile failure mechanisms are considered; on the other hand, the structural capacity decreases when brittle failure mechanisms are included. The evaluation method with consideration of the strain rate effect of the behaviour of RC structures under earthquake loading appears to be more proper.

The RC column is an elementary member of RC structures. The strain rate effect on the dynamic behaviour of RC columns by directly imparting rapid loading protocols has been partially studied. Reinschmidt et al. conducted several static and dynamic tests on plain and RC columns with a slenderness ratio (L/D) of 3 to 25 under eccentric or concentric axial loads [11]. They observed a 30-40 percent increase in the strength of columns under dynamic loads compared with the contrast columns under quasi-static loads, except the notably slender columns with a slenderness ratio of 25 were 70 to 100 percent stronger under dynamic loads than those tested under quasi-static loads. Xu and Zeng [12] found that the lateral inertial effect played an important role in increasing the axial bearing capacity for slender columns under axially rapid loading. Iwai et al. investigated the effect of the axial loading rate on the behaviour of RC columns [13]. Four short columns (L/D=6) and eight long columns (l/D=16 and 26) were tested under concentric and eccentric loads. The experimental results show that the maximum load of dynamically loaded columns is 11-14% larger than that statically loaded for concentric compression and 17- 37% larger under dynamic load for eccentric compression.

The aforementioned studies did not fully account for the confined effect of hoops under high strain rates. Under a static load, various studies show that the confined concrete behaves better than unconfined concrete. Then, the behaviour of confined concrete under dynamic loading becomes an interesting topic. To investigate the behaviour of concrete confined by hoops under rapid loading, Scott et al. conducted a test programme on twenty-five square short RC columns with different longitudinal steel bars and arrangements of overlapping hoops, which were subjected to concentric and eccentric loads at different strain rates [14]. The compressive strain rate was either 0.0000033/sec or 0.0167/sec. The test results show that a high longitudinal strain rate (0.0167/sec) increases the peak stress and descending branch of the core concrete by approximately 25%. A stress-strain curve for confined concrete loaded at a high strain rate was proposed by modifying Kent and Park's [15] stress-strain relation for confined concrete with a dynamic multiplying factor of 1.25 for the peak stress, strain at the peak stress and slope of the falling branch. Li et al. experimentally investigated the behaviour of short reinforced high-strength concrete columns [16]. Thirty specimens with different confining reinforcement configurations, yield strengths of transverse reinforcement and concrete compressive strengths, were tested under concentric loads at different strain rates (0.000011/sec and 0.0167/sec). The test results confirmed that high-strength concrete had lower strain rate sensitivity than low- and moderate-strength concrete. Under high strain rate loading, the modulus of elasticity and slope of the descending branch of the stress-strain curve increase, but the effect of the high strain rate on the compressive strength depends on the strength of the transverse reinforcement. Zeng and Xu [17] developed an FEA model in general-purpose finite element computer program ABAQUS to predict the behaviour of laterally confined short RC columns under rapid concentric loading, but the model had a shortcoming: the cover concrete and core concrete were simulated with the same identical constitutive models.

Despite two experimental programmes and limited numerical analyses that investigated the effects of the loading rates on RC columns confined by transverse reinforcement, the state of the art on the subject remains in its infancy. Until now, notably limited experimental data can be acquired to investigate the effect of different parameters at high strain rate, and there is notably little finite element modelling on the dynamic behaviour of RC columns. Because of the high requirement on loading instrument for the rapid loading test, the FEA modelling becomes a good choice for parametric studies. In this paper, the objective is to investigate the dynamic behaviour of square reinforced normal-strength concrete columns confined by overlapping hoops under rapid

concentric loading through finite element analysis. To model the behaviour of concrete confined by overlapping hoops (different from the hoops in the study by Zeng and Xu [17]) at high strain rates using the concrete damaged plasticity model in ABAQUS, a locally modified compressive stress-strain relation of concrete was developed based on the work by Zeng and Xu [17], which considers the confining effect of the overlapping hoops and strain rate effect of concrete. Then, an explicit dynamic FEA model was established in ABAQUS to evaluate and predict the behaviour of the overlapping-hoop-confined square reinforced normal-strength concrete columns with two different reinforcement arrangements (type A and type B, as shown in Figure 1). Finally, the effect of the parameters including the loading strain rate (3×10^{-5} - 3×10^{-1}/sec), reinforcement arrangement (type A and type B), longitudinal reinforcement ratios (ρ_s: 2.65% and 1.27%) and volumetric ratios of transverse reinforcement (ρ_{sv}: 3% and 1.5%) on the dynamic behaviour of confined RC columns was investigated.
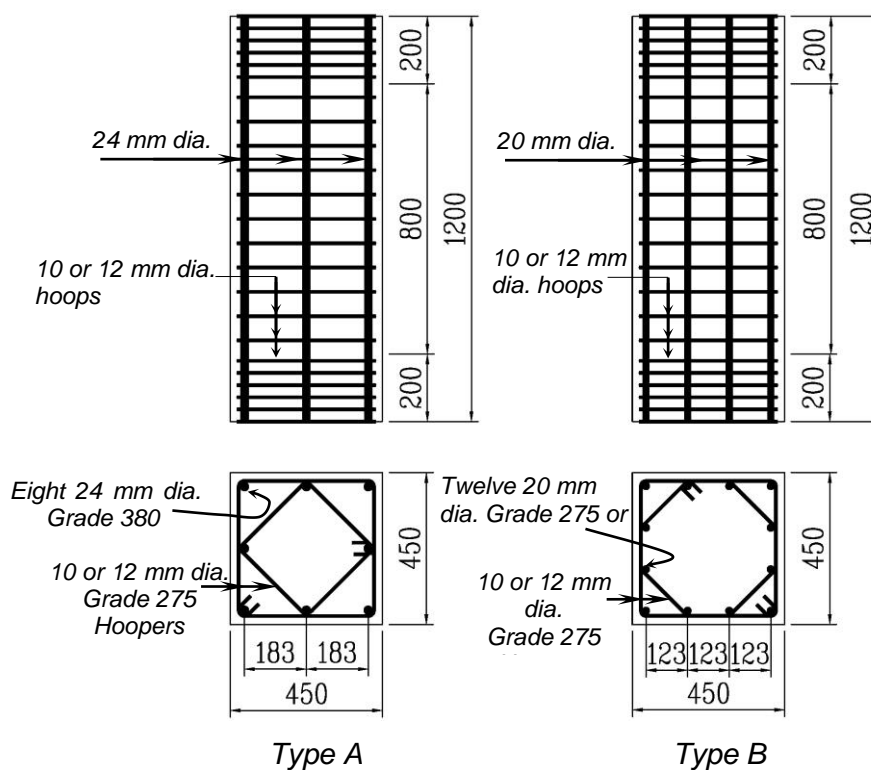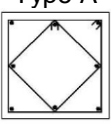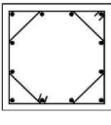

Fig. 1 - Typical details of the test units

BRIEF DESCRIPTION OF THE RAPID AXIAL LOADING EXPERIMENT ON RC COLUMNS

Until now, the experimental data of square reinforced normal-strength concrete columns confined by overlapping hoops under axial rapid loading have been notably limited and can only be acquired from literature [14]. In the paper, eight RC columns confined by overlapping hoops from the rapid concentric loading experiment of Scott et al. [14] were used to verify the following FEA model. Figure 1 shows that all test specimens have identical cross sections of 450 mm × 450 mm and are 1200 mm high. The longitudinal concrete strains in the test units were measured over the central 400-mm gage length of the units. Two reinforcement arrangements (type A and type B, as shown in Figure 1) were used. These arrangements are typical for 8-bar and 12-bar columns. The centre-to-centre spacing of longitudinal bars across the section for type-A and type-B arrangements was 183 mm and 123 mm, respectively. More details of the cross-sections in the test regions of different columns are shown in Table 1. The volumetric ratio of transverse

reinforcement ρ_{sv} is 0.0134 to 0.0309. The spacing of transverse hoops was reduced by one-half for 200 mm at each end of the test columns to provide extra confinement and ensure that failure occurred in the 800-mm-long central region. For columns under rapid concentric loadings, the strain rate was 0.0167/sec, which is representative of that expected during seismic loading. The quasi-static test columns with a strain rate of 0.0000033/sec were used for contrast.

Tab. 1 - Details of the cross-section of test columns

Specimens	Type of load	Reinforcement arrangement	Concrete compressive cylinder strength f_c (Mpa)	Longitudinal reinforcement			Transverse reinforcement			
				Number of bars	Diameter (mm)	Yield strength f_y (Mpa)	Diameter (mm)	Spacing (mm)	Yield strength f_{hy} (Mpa)	Volumetric ratio ρ_{sv}
Unit6	Quasi-static	Type A	25.3	8	24	394	10	72	309	0.0174
Unit7	Rapid loading		25.3				10	72	309	0.0174
Unit17			24.8				10	98	309	0.0134
Unit19			24.8				12	88	296	0.0213
Unit20			24.8				12	64	296	0.0293
Unit2	Quasi-static	Type B	25.3	12	20	434	10	72	309	0.0182
Unit3	Rapid loading		25.3				10	72	309	0.0182
Unit12			24.8				10	98	309	0.014
Unit14			24.8				12	88	296	0.0224
Unit15			24.8				12	64	296	0.0309

EXPLICIT DYNAMIC FEA MODELLING

To avoid numerical difficulty in convergence, the analysis module ABAQUS/Explicit was used to solve the quasi-static and dynamic analysis of RC columns under concentric loading.

The steel rebar was modelled using a 2-node linear 3D truss element (T3D2) in the explicit element library. The concrete was modelled using 8-node brick elements (C3D8R) in the explicit element library with three translational degrees of freedom at each node. The approximate global mesh size of 50 mm was used to discretize the concrete body, which can provide a precise simulation result. The load plate was modelled with an analytical rigid part, which is reasonable to save the computing cost because the load plate of the test machine is sufficiently stiff.

An embedded region constraint was used to simulate the interaction between the steel bars and concrete, which embedded the steel bars (embedded elements) into the concrete (host elements). In other words, the translational degrees of freedom of the embedded node were constrained to the interpolated values of the corresponding degrees of freedom of the host element, but these rotations were not constrained by the embedding [18]. General contact in the explicit module was used to simulate the interaction between the surfaces of the rigid load plate and the end of the column, which combines a rough friction formulation for the tangential behaviour and a contact pressure model for the normal direction behaviour.

In Figure 2, a quarter model with symmetric boundaries on the X-Y plane and Y-Z plane was used based on the symmetry, which reduced the computation cost. In ABAQUS, the motion of the rigid load plate at the end of the column was constrained to the motion of a reference point, so the axial load was applied to the top reference point with an allowable translational motion in the direction Z and an allowable rotational motion around the X-axis. The boundary conditions in the FEA model were selected according to the actual experimental boundary conditions.

Concrete material model

The concrete damaged plasticity model [18] was used to simulate the behaviour of concrete. The constitutive model uses concepts of isotropic damaged elasticity in combination with isotropic tensile and compressive plasticity to represent the inelastic behaviour of concrete. The damaged
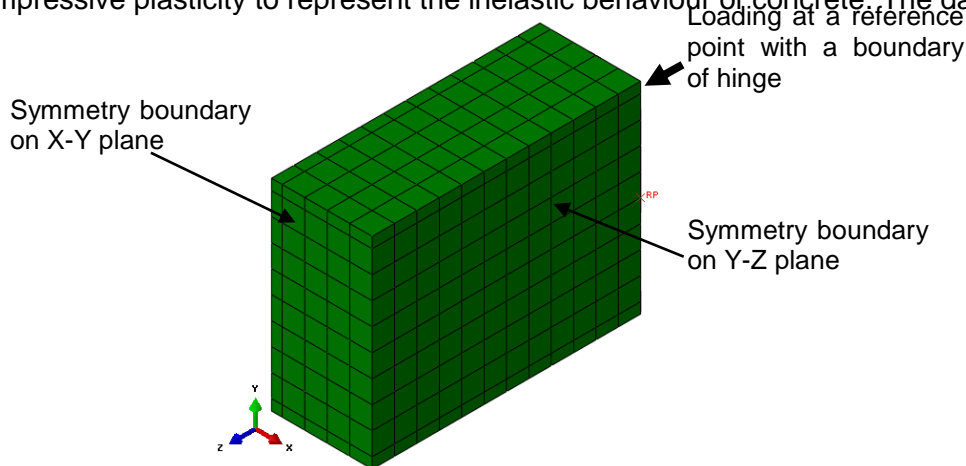

Fig. 2 - Illustration of the finite element model

model describes the irreversible damage that occurs during the fracturing process, which enables the user to control the stiffness recovery effects during cyclic load reversals. In this study, the test columns were under a monotonic load, there was no need to define the damaged model, and only the plasticity model was defined in the FEA model.

The plastic constitutive theory in the model is suitable to describe concrete and other quasi-brittle materials under fairly low confining pressures (less than four or five times the ultimate compressive stress in uniaxial compression loading) and can consider the strength improvement at the state of triaxial loading. It can also be defined as sensitive to the straining rate. The key parameters of the plasticity model are as follows: the dilation angle, eccentricity, ratio of the biaxial compression strength to the uniaxial compression strength of concrete, ratio of the second stress invariant on the tensile meridian to that on the compressive meridian and viscosity parameter are 30°, 0.1, 1.16, 0.667, and 0.0001, respectively [19]. Regarding the dynamic modulus of elasticity, Bischoff and Perry noted the confusion about whether the initial tangent modulus should change with the strain rate because of the confliction from different experimental results [2]. In this study, the modulus of elasticity is assumed to be constant for an effective numerical implementation in ABAQUS and is equal to $4730\sqrt{f_c}$ by ACI 318 [20], where f_c (N/mm^2) is the compressive cylinder strength of concrete under a quasi-static load. Poisson's ratio of concrete is assumed to be constant under dynamic loading, as recommended by CEB [21], and is equal to 0.2. Moreover, an equivalent uniaxial compressive stress-strain relationship and tension stiffening are required in the plasticity model of concrete, which will be described as follows.

Uniaxial compressive stress-strain relation of confined concrete considering the strain rate effect

As previously mentioned, the range of strain rate of the materials in RC structures under earthquake loading is approximately 10^{-4}/sec to 10^{-1}/sec [7-9]. To consider the strain rate sensitivity of concrete, the dynamic compressive cylinder strength f_{cd} of concrete can be estimated from Equations 1 and 2 provided by CEB-FIP Model Code 1990 [1].

$$f_{cd} / f_{cs} = (\frac{\dot{\varepsilon}}{\dot{\varepsilon}_{cs}})^{1.026\alpha_s} \qquad \dot{\varepsilon} \leq 30 s^{-1} \tag{1}$$

$$\alpha_s = \frac{1}{5 + 9 f_{cs} / f_{co}}$$ (2)

where f_{cs} is the quasi-static compressive strength of unconfined concrete; $f_{cs} = 0.85 f_c$ considering a strength-reduction factor related to the column shape, size and the difference between the strength of in situ concrete and the strength determined from standard cylinder tests [22-23]; $\dot{\varepsilon}$ is the strain rate (s⁻¹); $f_{co} = 10$ Mpa; and $\dot{\varepsilon}_{cs} = 30 \times 10^{-6}$ s⁻¹. f_{cd} increases with increasing strain rate; the other parameters in the following uniaxial compressive stress-strain curve correspondingly change, and the dynamic uniaxial compressive stress-strain curve is formed.

The uniaxial compressive stress-strain relation of confined concrete considering the strain rate effect is shown in Figure 3, which is suitable for the dynamic finite element analysis of concrete confined by overlapping hoops using ABAQUS. The basic equations (Equation 3 to 6) of the stress-strain relation, which were proposed by the author [17,19], are used.

$$y = \begin{cases} \alpha_a \cdot x + (3 - 2\alpha_a)x^2 + (\alpha_a - 2)x^3 & (x \le 1) \\ \dfrac{x}{\alpha_d \cdot (x-1)^2 + x} & (x > 1) \end{cases}$$ (3)

$$x = \frac{\varepsilon}{\varepsilon_{co}} \; ; \quad y = \frac{\sigma}{f_{cd}}$$ (4)

$$\alpha_a = 2.4 - 0.0125 f_{cd}$$ (5)

$$\alpha_d = \frac{\varepsilon_{cc50}/\varepsilon_{co}}{(\varepsilon_{cc50}/\varepsilon_{co} - 1)^2}$$ (6)

where parameters α_a and α_d control the slope of the ascending and descending branches of the stress-strain curve, respectively; ε and σ are the strain and stress of the confined concrete under dynamic loading, respectively; and ε_{co} is the peak strain of the confined concrete (as shown in Figure 3), which is expressed as [17]

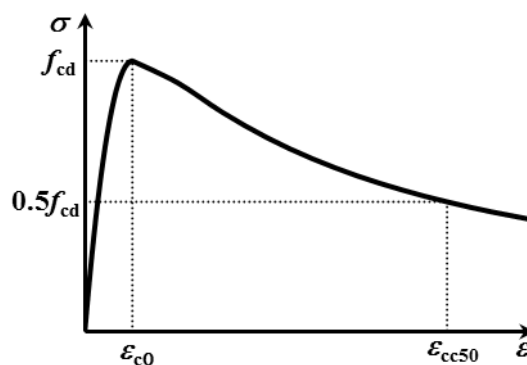$$\varepsilon_{co} = (1300 + 12.5 \cdot \sigma_{co}) \cdot 10^{-6} + 800 \cdot \xi^{0.2} \cdot 10^{-6}$$ (7)

Fig. 3 - Dynamic stress-strain relation of confined concrete

where $\xi = \rho_{sv} f_h / f_{cd}$, ρ_{sv} is the volume ratio of the transverse hoop to the confined concrete core, and f_h is the stress in confinement reinforcement at the peak strength of confined concrete. f_h was proposed by Le'geron and Paultre [23] as follows:

$$f_h = \begin{cases} f_h = f_{hy} & \kappa \le 10 \\ f_h = \min\left(f_{hy}, \dfrac{0.25 f_{cd}}{\rho_{se}(\kappa - 10)} \right) & \kappa > 10 \end{cases}$$ (8)

----

where f_{hy} is the yield strength of stirrups; ρ_{se} is the effective sectional ratio of confinement reinforcement in the x or y direction (Figure 4); and κ is a parameter to determine whether the transverse reinforcement yields at the peak strength of confined concrete. ρ_{se} and κ are expressed as follows:

$$\rho_{se} = k_e A_{sh}/sc \tag{9}$$

$$\kappa = f_{cd}/(\rho_{se}E_s\varepsilon_c) \tag{10}$$

where s and c (as shown in Figure 4, $c=c_x=c_y$) are the spacing of transverse reinforcement and diameter of the core measured centre-to-centre of the hoops, respectively; A_{sh} is the total area of transverse bars in the x or y direction and is defined as 3.41 and 3.61 times the cross-section area of a single tie leg for the type-A and type-B configurations in Table 1, respectively [24]; E_s and ε_c are the modulus of elasticity of transverse reinforcement and the axial strain, which corresponds to the concrete cylinder strength, respectively; and k_e is the geometrical effectiveness coefficient of confinement, which represents the ratio of the smallest effectively confined concrete area at midway between two layers of stirrups to the nominal concrete core area. k_e was proposed by Mander et al. [25] as follows:

$$k_e = \frac{(1 - \frac{\sum w_i^2}{6c_x c_y})(1 - \frac{s'}{2c_x})(1 - \frac{s'}{2c_y})}{1 - \rho_c} \tag{11}$$

where w_i is the ith clear distance between adjacent longitudinal bars (as shown in Figure 4); s' is the clear spacing of transverse reinforcement; ρ_c is the ratio of the area of longitudinal steel to the area of the core of the section; and c_x and c_y are the core dimensions to centrelines of the perimeter hoop in the x and y directions, respectively.

In Equation 4, ε_{cc50} is the post-peak axial strain in confined concrete when the capacity decreases to 50% of the confined strength. Based on the expression of ε_{cc50} proposed by Le´geron and Paultre [23], the modified expression of ε_{cc50} is

$$\varepsilon_{cc50} = \varepsilon_{c50}(1 + 40I_{e50}) \tag{12}$$

where ε_{c50} is the post-peak axial strain in unconfined concrete under quasi-static load when the capacity decreases to 50% of unconfined strength, and $\varepsilon_{c50}=0.004$ according to the proposal of Le´geron and Paultre [23]; I_{e50} is the effective confinement index at ε_{cc50},

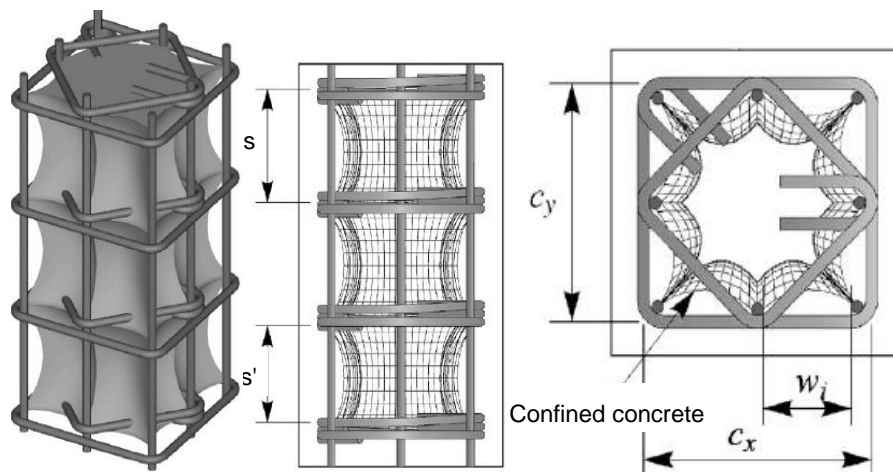$$I_{e50} = \rho_{se}f_{hy}/f_{cd} \tag{13}$$

Fig. 4 - Diagram of the partial parameters [26]

Uniaxial compression stress-strain relations of cover concrete considering the strain rate effect

When the volume ratio of transverse steel is $\rho_v = 0$ and the effective confinement index is $I_{e50} = 0$ in Equations 7 and 10, respectively, Equation 1 to 13 describe the uniaxial compressive stress-strain relation of cover concrete with the strain rate effect, which can be used to analyse the behaviour of the cover concrete of RC columns.

Uniaxial tensile behaviour

In ABAQUS, the uniaxial tensile behaviour of concrete is taken as a linear elastic relation before reaching the tensile strength [18]. The post-failure behaviour for direct straining is modelled with tension stiffening, which enables the user to define the strain-softening behaviour for cracked concrete. This behaviour also enables the effects of the reinforcement interaction with concrete to be simulated in a simple manner. One method to specify tension stiffening is applying a fracture energy cracking criterion. The fracture energy is directly specified as a material property in the model, and a linear loss of strength after cracking is assumed. The fracture energy G_F in N/m is determined by the expression proposed by the *Fib Model Code for Concrete Structures 2010* [27],

$$G_F = 73 f_c^{0.18} \tag{14}$$

where f_c is the compressive strength in MPa.

As suggested by available studies [28-30] on the dynamic fracture energy of concrete, the dynamic fracture energy of concrete can be assumed to be identical to the static fracture energy for the strain rate range from 10^{-4} to 10^{-1} under earthquake action.

Steel material model

An isotropic elastic-plastic model was used to describe the constitutive behaviour of the steel bar. The perfect elastic-plastic relation was used as the uniaxial stress-strain relation of steel. Based on the studies on the dynamic behaviour of steel, the steel modulus of elasticity has no relation to the strain rate. The steel modulus of elasticity is constant under dynamic loading. The dynamic yield strength of steel σ_{yd} is obtained using the Cowper-Symond equation,

$$\frac{\sigma_{yd}}{\sigma_{ys}} = 1 + \left(\frac{\dot{\varepsilon}}{C}\right)^{1/q} \tag{15}$$

where σ_{ys} is the static yield strength of steel, $\dot{\varepsilon}$ is the strain rate of steel, $C=1300$ s^{-1} and $q=5$ according to Munoz-Garcia et al. [31].

VERIFICATION OF FEA MODEL

Based on the FEA model, the quasi-static and dynamic behaviours of the columns in Table 1 were simulated. Figures 5 and 6 show that the predicted axial load (N) versus the axial strain (ε) curves are consistent with the tested N-ε curves under the conditions of quasi-static loading and rapid loading. Because the available tested N-ε curves under rapid loading from the literature are notably limited, the comparison between the predicted N-ε curves and the tested axial bearing capacity are shown in Figures 5 and 6. Table 2 shows the comparison between experimental and predicted axial bearing capacities (P_e and P_c) and the corresponding average axial strain (ε_c and ε_e). The largest error of the predicted axial bearing capacity is 7% for Unit19. The mean value and standard deviation of P_c/P_e are 0.97 and 0.03, respectively. The largest error of the predicted axial strain at the bearing capacity is 36% for Unit12, but the mean value and standard deviation of $\varepsilon_c/\varepsilon_e$ are 1.11 and 0.16, respectively. The comparison shows that the FEA model is effective to predict the quasi-static and dynamic behaviour of square reinforced normal-strength concrete columns with different volume ratios of transverse reinforcement.
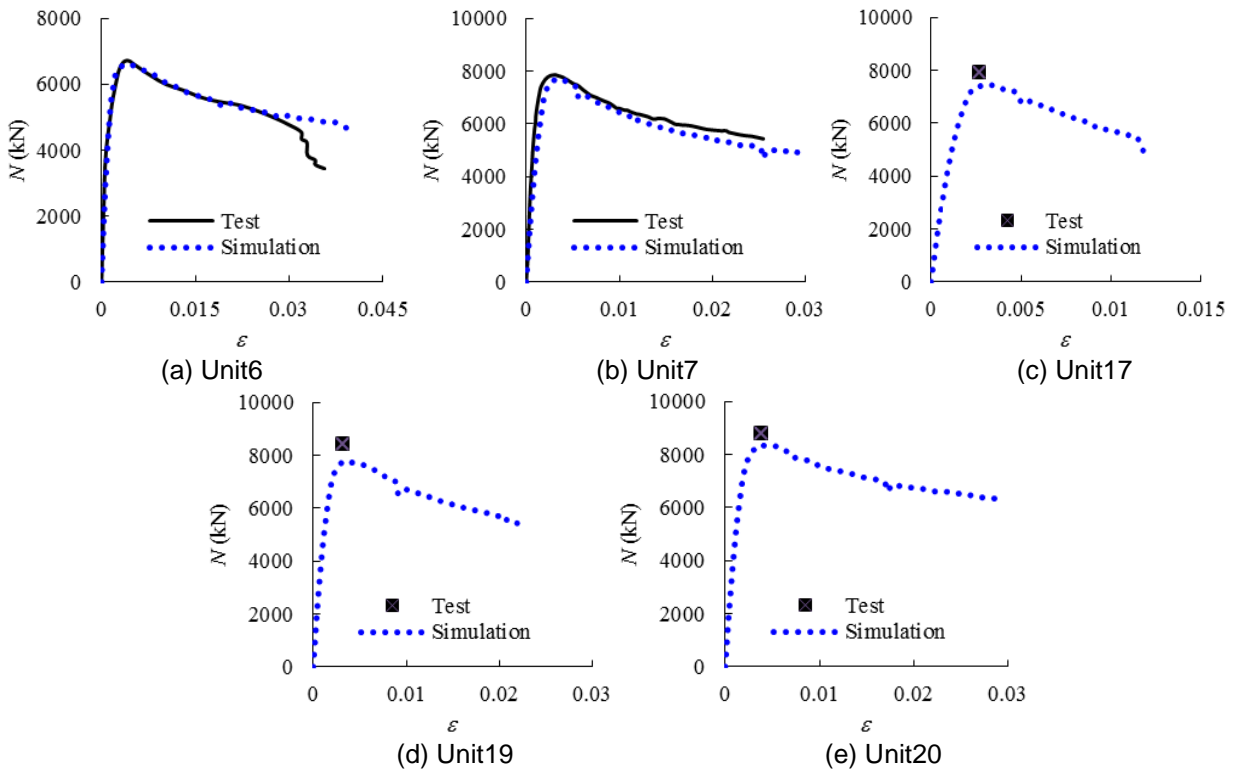

(a) Unit6

(b) Unit7

(c) Unit17

(d) Unit19

(e) Unit20

Fig. 5 - Comparison between experimental and predicted N-ε curves of columns with type-A reinforcement arrangement

(a) Unit2

(b) Unit3

(c) Unit12

(d) Unit14

(e) Unit15

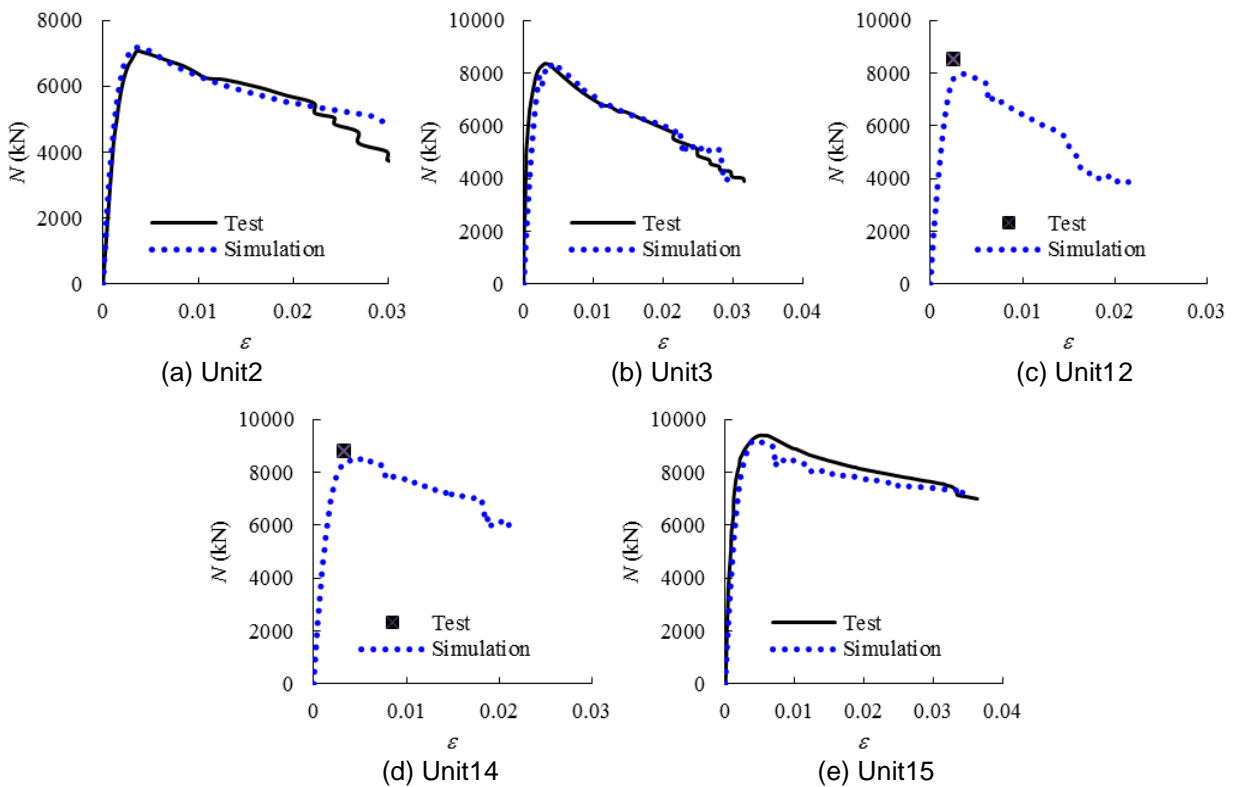*Fig. 6 - Comparison between experimental and predicted N-ε curves of the columns with type-B reinforcement arrangement*

Tab. 2 - Comparison between tested and predicted bearing capacities and the corresponding axial strain

Specimens	P_e/kN	P_c/kN	P_c/P_e	ε_e	ε_c	$\varepsilon_c/\varepsilon_e$
Unit6	6720	6628	0.99	0.0041	0.0041	1.00
Unit7	7850	7717	0.98	0.0032	0.0035	1.09
Unit17	7900	7455	0.94	0.0027	0.0032	1.19
Unit19	8400	7794	0.93	0.0032	0.0034	1.06
Unit20	8800	8362	0.95	0.0039	0.0037	0.95
Unit2	7070	7175	1.01	0.0036	0.0035	0.97
Unit3	8410	8360	0.99	0.003	0.0038	1.27
Unit12	8500	7974	0.94	0.0025	0.0034	1.36
Unit14	8800	8532	0.97	0.0033	0.0042	1.27
Unit15	9400	9188	0.98	0.0052	0.0047	0.90
Mean			0.97			1.11
Standard deviation			0.03			0.16

Note: P_e and P_c are the experimental and simulation axial-bearing capacity, respectively; ε_e and ε_c are the experimental and simulation axial strain at the axial-bearing capacity, respectively.

PARAMETRIC INVESTIGATION

Numerical simulation matrix

After the verification of the FEA model against the experimental results, this section presents a parametric investigation to capture more information about the behaviour of RC columns under varying loading rates. Various key parameters were considered, including the loading strain rate (3×10^{-5}, 3×10^{-4}, 3×10^{-3}, 3×10^{-2} and 3×10^{-1} s^{-1}), reinforcement arrangement (type A and type B), longitudinal reinforcement ratios (ρ_s: 2.65% and 1.27%) and volumetric ratios of transverse reinforcement (ρ_{sv}: 3.0% and 1.5%). Table 3 summarizes the specimen characteristics of the simulation matrix. The titles of the specimens in Table 3 describe the varying parameters and have the following meaning. The first letter (A or B) in the titles represents the reinforcement arrangement of type A or type B. The number after the first letter indicates the ratio of longitudinal steel ρ_s. Numbers 2 and 1 correspond to ρ_s=2.65% and ρ_s=1.27%, respectively. The numbers behind the middle hyphen represent the volumetric ratio ρ_{sv} of the transverse reinforcement. Numbers 3.0 and 1.5 indicate ρ_{sv}=3% and ρ_{sv}=1.5%, respectively. All specimens are 1200 mm long and have identical section sizes of 450 mm × 450 mm. The core size measured from the centre of the perimeter hoop was maintained constant at 400 mm × 400 mm. The concrete compressive cylinder strength f_c was 30 MPa.

Influence analysis of investigated parameters

As shown in Figure 7, the loading rate has an obvious effect on the N-ε curves. First, the axial bearing capacity increases with the increase in loading rate. The dynamic increasing factor (*DIF*) of the bearing capacity, namely, the ratio of dynamic bearing capacity to quasi-static bearing capacity at a strain rate of 0.000033/sec, is commonly used to describe the effect of the loading rate on the bearing capacity. In these cases, the maximum *DIF* is 1.28 for specimen A1-1.5 when the strain rate increases to 0.3/sec. Second, the ductility obviously decreases after the loading rate increases. The descending branches of N-ε curves with different loading rates appear to converge

----

after the axial strain ε reaches a certain value.

Tab. 3 - Specimens for the parameter analysis

Specimen	Longitudinal reinforcement			Transverse reinforcement			
	Diameter (mm)	Ratio of longitudinal steel ρ_s	Yielding strength f_y (Mpa)	Diameter (mm)	Spacing (mm)	Yielding strength f_{hy} (MPa)	Volumetric ratio ρ_{sv}
A1-3.0	18	1.27%	400	10	43	300	3.0%
A1-1.5	18	1.27%	400	10	86	300	1.5%
A2-3.0	26	2.65%	400	10	43	300	3.0%
A2-1.5	26	2.65%	400	10	86	300	1.5%
B1-3.0	14.7	1.27%	400	9.7	43	300	3.0%
B1-1.5	14.7	1.27%	400	9.7	86	300	1.5%
B2-3.0	21.2	2.65%	400	9.7	43	300	3.0%
B2-1.5	21.2	2.65%	400	9.7	86	300	1.5%

(a) A2-3.0

(b) A2-1.5

(c) A1-3.0

(b) A1-1.5
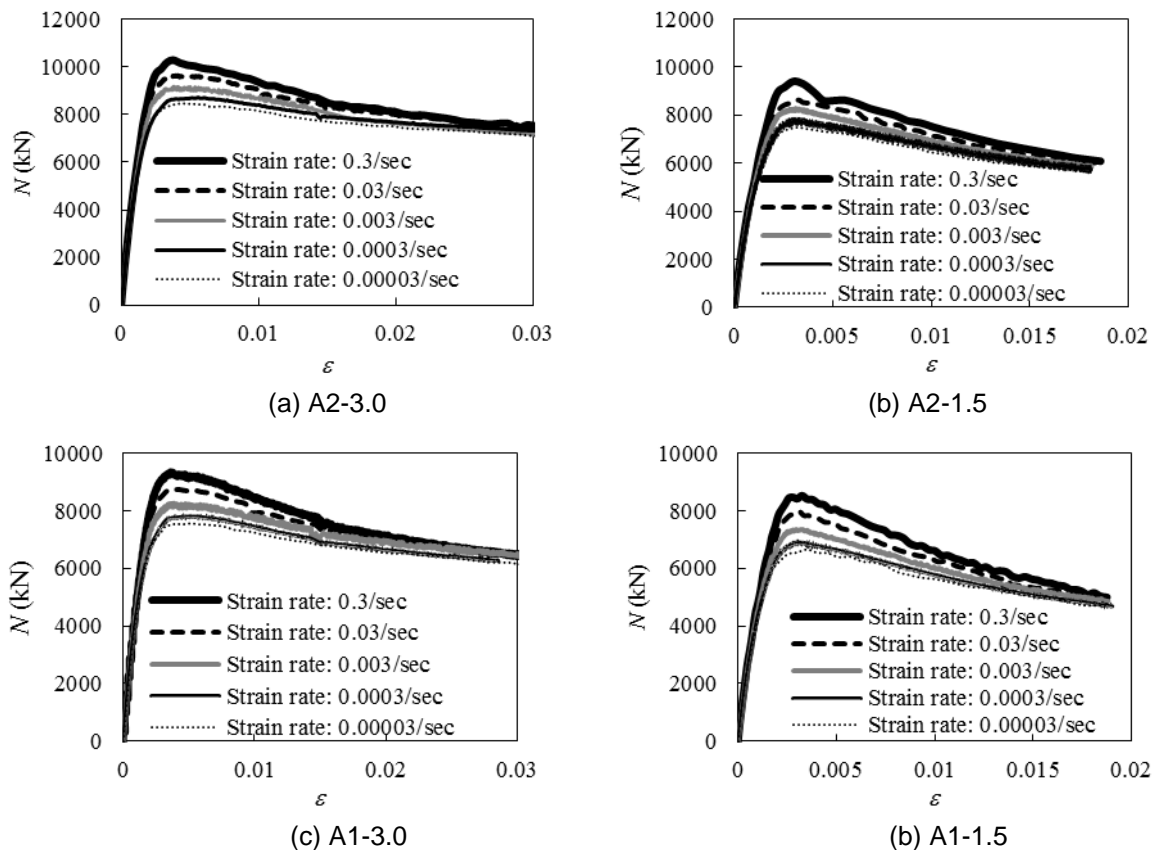
Fig. 7 - Effect of the loading rate on the N-ε curves

Figure 8 shows the effect of the transverse reinforcement volumetric ratio (ρ_{sv}: 3.0% and 1.5%) on the *DIF*. Improving the transverse reinforcement volumetric ratio reduces the *DIF*. With the increase in strain rate, the difference of the *DIF* with two different volumetric ratios of

transverse reinforcement increases. Compared with the specimens with type-A reinforcement arrangement, the difference of *DIF* with different volumetric ratios of transverse reinforcement is more obvious for the specimens with type-B reinforcement arrangement. However, the maximum difference of *DIF* is only 5.3%, which is notably small. Thus, the effect of the transverse reinforcement volumetric ratio in the range of 1.5% to 3% on the *DIF* can be ignored.
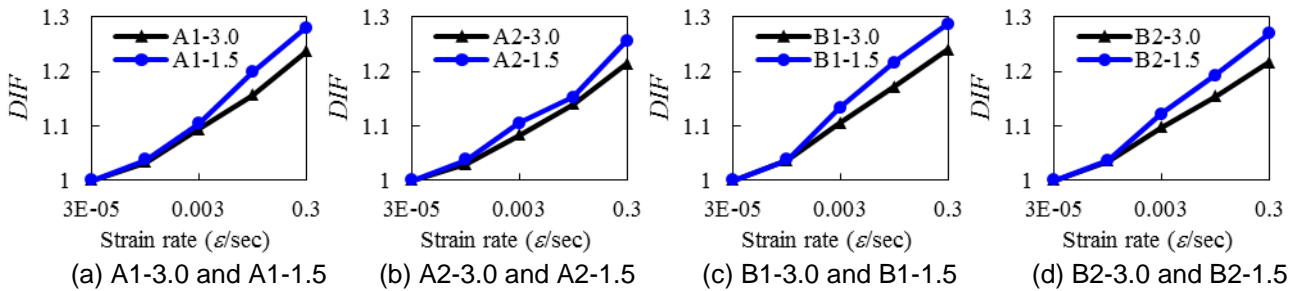

Fig. 8 - Effect of the transverse reinforcement ratio on DIF

Figure 9 shows that an increase in longitudinal reinforcement ratio from 1.27% to 2.65% makes the *DIF* slightly decrease. Figure 10 shows the effect of the reinforcement arrangement on the *DIF*. The two specimens in each group in Figure 10 have identical longitudinal reinforcement ratio and transverse reinforcement volumetric ratio but different reinforcement arrangements. The *DIF* of specimens with type-B reinforcement arrangement is slightly larger than the *DIF* of specimens with type-A reinforcement arrangement. In sum, the effect of the longitudinal reinforcement ratio and reinforcement arrangement on *DIF* is smaller than the effect of the transverse reinforcement ratio, and the effect is also commonly negligible.
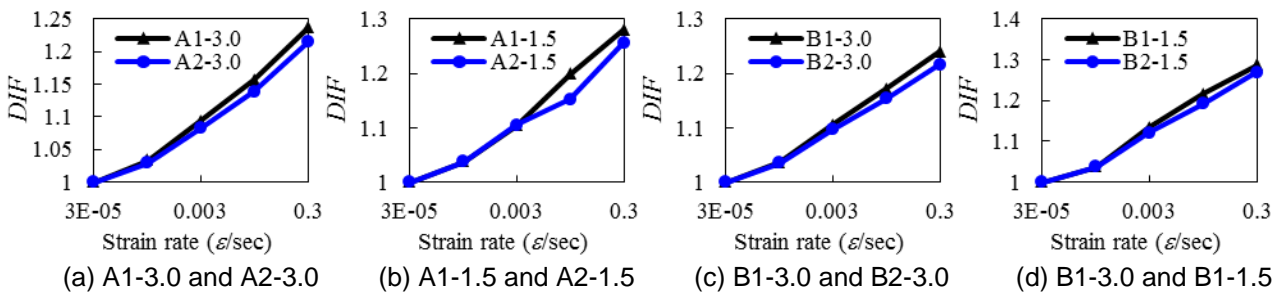

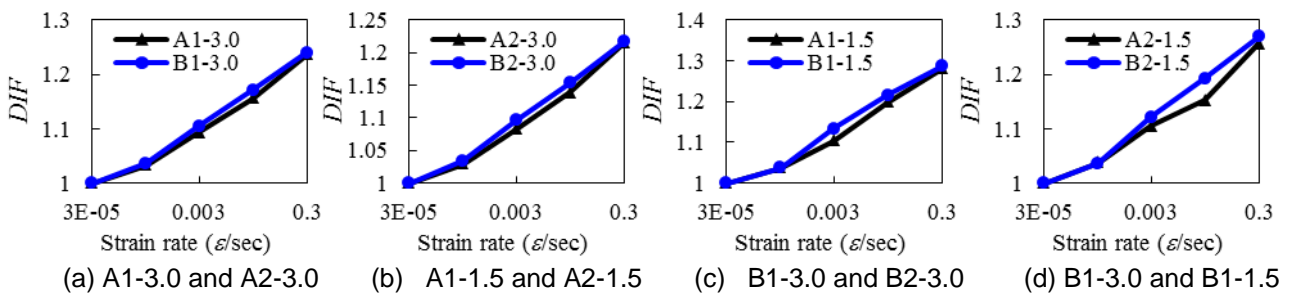*Fig. 9: Effect of the longitudinal reinforcement ratio on DIF*

Fig. 10: Effect of the reinforcement arrangement on DIF

CONCLUSION

In this paper, a three-dimensional FEA model was developed to investigate the behaviour of RC columns with the overlapping hoop confining effect under different concentric loading rates. The predicted results by the FEA model were consistent with the test results. Based on the numerical results obtained in the study, the following conclusions were drawn.

(1) A modified uniaxial compressive stress-strain relation of concrete was developed, including the confining effect of overlapping hoops and strain rate effect of concrete, and it is proper to simulate the quasi-static and dynamic behaviour of the overlapping hoop-confined concrete by introducing it into the concrete damaged plastic material model in ABAQUS.

(2) Increasing the loading rate increases the axial bearing capacity but decreases the ductility of RC columns. Compared with the quasi-static bearing capacity, the increase in axial bearing capacity is obvious when the strain rate approaches 0.3/sec.

(3) For the RC columns with the reinforcement arrangement of type A or type B, the transverse reinforcement volumetric ratio and longitudinal reinforcement ratio slightly affect the *DIF* of specimens under the strain rate of 0.00003/sec to 0.3/sec.

(4) With the identical volumetric ratio of transverse reinforcement and longitudinal reinforcement ratio, the change of reinforcement arrangement between type A and type B slightly affects the *DIF* of specimens under the strain rate of 0.00003/sec to 0.3/sec.

ACKNOWLEDGEMENTS

REFERENCES

[1]   Comité Euro-International du Béton, 1993. CEB-FIP Model Code 1990 (Redwood Books).

[2]   Bischoff P.H., Perry S.H., 1991. Compressive behaviour of concrete at high strain rates. Materials and Structures, 24(6): 425-450. http://dx.doi.org/10.1007/BF02472016.

[3]   Malvar L.J., Ross C.A., 1998. Review of strain rate efects for concrete in tension. ACI Materials Joumal, 95(6): 735-739.

[4]   Fu H.C., Erki M.A., Seckin M., 1991. Review of effects of loading rate on reinforced concrete. Journal of Structural Engineering, 117(12): 3660-3679. http://dx.doi.org/10.1061/(ASCE)0733-9445(1991)117: 12(3660).

[5]   Malvar L.J., Ross C.A., 1998. Review of static and dynamic properties of steel reinforcing bars. ACI Materials Journal, 95(5): 609-616.

[6]   Bertero V.V., 1972. Experimental studies concerning reinforced, prestressed and partially prestressed concrete structures and their elements. Introductory Report, Symposium on Resistance and Ultimate Deformability of Structures Acted on by Well Defined Repeated Loads, 67-99.

[7]   Soroushian P., Obaseki K., 1986. Strain rate-dependent interaction diagram for reinforced concrete section. ACI Journal Proceedings, 83(1): 108-116.

[8]   Al-Haddad M.S., 1995. Curvature ductility of reinforced concrete beams under low and high strain rates. ACI Structural Journal, 92(5): 526-534.

[9]   Lin G., Yan D.M., Xiao S.Y., Hu Z.Q., 2005. Strain rate effects on the behavior of concrete and the seismic response of concrete structures. China Civil Engineering Journal, 38(11): 1-8.

[10]   Asprone D., Frascadore R., Ludovico M.D., Prota A., Manfredi G., 2012. Influence of strain rate on the seismic response of RC structures. Engineering Structures, 35: 29-36. http://dx.doi.org/10.1016/j.engstruct.2011.10.025.

[11]   Reinschmidt K.F., Hansen R.J., Yang C.Y., 1964. Dynamic tests of reinforced concrete columns. ACI Journal Proceedings, 61(3): 317-334.

[12]   Xu B., Zeng X., 2014. Experimental study and finite element analysis on the dynamic

----

behavior of slender RC columns under concentric compressive rapid loadings. Engineering Mechanics, 31(4): 210-217.

[13]   Iwai S., Minami K., Wakabayashi M., 1988. Stability of slender reinforced concrete members subjected to static and dynamic loads. In: Proceedings of Ninth World Conference on Earthquake Engineering, Vol. Ⅷ 901-906.

[14]   Scott B.D., Park R., Priestley M.J.N., 1982. Stress-strain behavior of concrete confined by overlapping hoops at low and high strain rates. ACI Journal Proceedings, 79(1): 13-27.

[15]   Kent D.C., Park R., 1971. Flexural members with confined concrete. Journal of the Structural Division, 97(7): 1969-1990.

[16]   Li B., Park R., Tanaka H., 2000. Constitutive behavior of high-strength concrete under dynamic loads. ACI Structural Journal, 97(4): 619-629.

[17]   Zeng X., Xu B., 2014. Numerical simulation on the dynamic behavior of short RC columns subjected to concentric rapid loading considering confinement effect of stirrups. Engineering Mechanics, 31, 190-197.

[18]   Dassault Systemes Simulia Corp., 2014. Abaqus Version 6.14 Documentation- ABAQUS Theory Guide (Dassault Systemes Simulia Corporation).

[19]   Zeng X., 2016. Finite element modelling and analysis of concrete confined by stirrups in square RC columns. The Civil Engineering Journal, 3: Article no. 17. https://doi.org/10. 14311/CEJ.20 16.03.0 017.

[20]   ACI Committee 318, 2008. Building code requirements for structural concrete (ACI 318-08) and commentary (American Concrete Institute) 109 pp.

[21]   CEB, 1988. Concrete Structures under Impact and Impulsive Loading. Synthesis Report, Bulletin d'Information No. 187 (Comité Euro-International du Béton).

[22]   Chung H.S., Yang K.H., Lee Y.H., Eun H.C., 2002. Strength and ductility of laterally confined concrete columns. Canadian Journal of Civil Engineering, 29(6): 820-830. http://dx.doi.org/10.1139/l02-084.

[23]   Le´geron F., Paultre P., 2003. Uniaxial confinement model for normal- and high-strength concrete columns. Journal of Structural Engineering, 129(2): 241-252. http://dx.doi.org/10.1061/(ASCE)0733-9445(2003)129:2(241).

[24]   Cusson D., Paultre P., 1995. Stress-strain model for confined high-strength concrete. Journal of Structural Engineering, 121(3): 468-477. http://dx.doi.org/10.1061/(ASCE)0733-9445(1995)121:3(468).

[25]   Mander J.B., Priestley M.J.N., Park R., 1988. Theoretical stress-strain model for confined concrete. Journal of Structural Engineering, 114(8): 1804-1826. http://dx.doi.org/10.1061/(ASCE)0733-9445(1988)114:8(1804)

[26]   Paultre P., Légeron F., 2008. Confinement reinforcement design for reinforced concrete columns. Journal of Structural Engineering, 134(5): 738-749. http://dx.doi.org/10.1061/(ASCE)0733-9445(2008)134:5(738).

[27]   Fib, 2013. Fib Model Code for Concrete Structures 2010 (Ernst & Sohn).

[28]   Van Doormaal J., Weerheijm J., Sluys L.J., 1994. Experimental and numerical determination of the dynamic fracture energy of concrete. Journal de Physique IV, 4(C8): 501-506.

[29]   Rericha P.A., 1998. Structures Under Shock and Impact V, edited by Jones N., Talaslidis D.G., et al. (Computational Mechanics Publications in Southampton, Boston) 461-470.

[30]   Ruiz G., Zhang X.X., Yu R.C., et al., 2011. Effect of loading rate on fracture energy of high-strength concrete. Strain, 47(6): 518-524. http://dx.doi.org/10.1111/j.1475-1305.2010.00719.x.

[31]   Munoz-Garcia E., Davison B., Tyas A., 2005. Structural integrity of steel connections subjected to rapid rates of loading. In: Structures Congress 2005: Metropolis and Beyond, 1-12. http://dx.doi.org/10.1061/40753(171)217.